

RESEARCH PAPER

Graphene Oxide-terpyridine Conjugate: A Highly Selective Colorimetric and Sensitive Fluorescence Nano-chemosensor for Fe²⁺ in Aqueous Media

Bagher Eftekhari-Sis* and Somayeh Mirdoraghi

¹ Department of Chemistry, University of Maragheh, Maragheh, Iran

ARTICLE INFO

Article History:

Received 30 January 2016

Accepted 4 June 2016

Published 1 July 2016

Keywords:

Chemosensor

Colorimetric

Fe

Fluorescence

Graphene oxide

Nanosensor

Terpyridine

ABSTRACT

A graphene oxide-terpyridine conjugate (GOTC) based colorimetric and fluorescent nano-chemosensor was synthesized. It showed high selectivity and sensitivity for Fe²⁺ and Fe³⁺ ions in neutral aqueous solution over other metal ions such as Li⁺, Na⁺, Ba²⁺, Ca²⁺, Al³⁺, Cd²⁺, Co²⁺, Cu²⁺, Hg²⁺, Mn²⁺, Ni²⁺, Pb²⁺, Zn²⁺, Cr³⁺ and Ag⁺. In absorption spectra, upon addition of Fe²⁺ or Fe³⁺, the sensor displayed a peak at 568 nm, by changing the color of the solution from light pink for GOTC to light magenta and deep magenta for Fe³⁺ and Fe²⁺, respectively. Also, the fluorescence studies revealed that, Fe²⁺, Fe³⁺ and Co²⁺ quench the emission of GOTC at 473 nm, while other metal ions do not quench the fluorescence of GOTC in solution. Colorimetric and fluorescence techniques could be used for detection of Fe²⁺ ion concentration at least about 6-10 μM in water solution. The sensing on test paper was also investigated for the naked-eye detection of Fe²⁺.

How to cite this article

Eftekhari-Sis B, Mirdoraghi S. Graphene Oxide-terpyridine Conjugate: A Highly Selective Colorimetric and Sensitive Fluorescence Nano-chemosensor for Fe²⁺ in Aqueous Media. *Nanochem Res*, 2016; 1(2): 214-221. DOI: 10.7508/ncr.2016.02.008

INTRODUCTION

The design and development of new materials for the recognition and sensing of transition-metal ions in aqueous solution have received great attention in environmental chemistry and biology [1-4]. In particular, colorimetric methods are of interest because they allow naked-eye detection of color change without any use of a complicated analytical instrument [5-9]. Also, due to their convenient use, high sensitivity, and real-time detection, a tremendous attention has been paid to the development of fluorescent chemo sensors for metal ions [10-15].

Iron is the most abundant intracellular metal ion and one of the most essential trace elements in biological systems. It is an essential element for the formation of hemoglobin and various enzymes in the human body [16] and plays crucial role in

many biological processes [17-19], and deficiencies or excesses of iron ions cause a variety of diseases [20]. Therefore, the development of sensitive and selective sensors for iron ions is of considerable interest. Although, examples of colorimetric and fluorescent chemical sensors for Fe³⁺ were reported [21-26], which most of them rely on small organic molecules with low solubility in water having no application for iron ion detection in biological environments, there are only a few fluorescent sensors reported for Fe²⁺ until now [27,28].

Terpyridine ligands have not been generally used for sensors, due to possessing an excellent ability to coordinate with a large variety of transition metal ions with high binding constants. However, there are some limited reports on the sensing of iron metal ions by terpyridine containing sensors. In this context, Liang *et al.* reported a colorimetric

* Corresponding Author Email: eftekharis@maragheh.ac.ir

chemosensor containing terpyridine moiety for Fe²⁺ and Fe³⁺ ions in aqueous solution [29]. Also, a europium-based metal-organic framework (Eu-MOF), EuL₃ (L = 4'-(4-carboxyphenyl)-2,2':6,2''-terpyridine), was reported as a luminescence sensor for Fe³⁺ ions [30].

Graphene oxide (GO), a highly dispersed derivative of graphene in water, has found important applications, especially in sensors for detecting DNA [31-34], small molecules [35,36], proteins [37], and cells [38], because of its distinguished electronic properties [39,40]. In continuing our research on the sensors [41], herein we wish to report a new graphene oxide-terpyridine conjugate for the selective and sensitive recognition of Fe²⁺ ion in aqueous solution.

EXPERIMENTAL

Materials and Apparatus

All chemicals were purchased from Merck and Sigma-Aldrich and used without any further purification. Solvents were used as received from commercial suppliers. FT-IR spectra were obtained using a Perkin Elmer 781 spectrometer. UV-Vis spectra were recorded using Shimadzu UV-1800 spectrophotometer and fluorescence spectra were measured using JASCO-FP-750, Rev. 1.00 fluorometer. TEM images were recorded using a Philips CM120 microscope. SEM images were recorded using a MIRA3 TESCAN microscope.

Synthesis of 4'-(4-(hydroxyethoxy)phenyl)-2,2':6,2''-terpyridine 3. A mixture of chloroethanol (41 mmol, 3.3 g), 4-hydroxybenzaldehyde 1 (41 mmol, 5.0 g) and Na₂CO₃ (56 mmol, 5.9 g) in 15 ml DMF was heated under reflux conditions for 24 h. Then, water was added and extracted by EtOAc three times. The combined organics were dried over anhydrous MgSO₄ and evaporated to give 4-(2-hydroxy-ethoxy)benzaldehyde 2 as a yellow viscous oil [42], which was used in next step without further purification. Obtained 2 and 2-acetylpyridine (105 mmol, 12.7 g) were dissolved in 600 ml MeOH/dioxane (1/1; v/v) mixture, and stirred at 50 °C for 5 min. Then, 40 ml NH₃·H₂O and 240 ml NaOH (15% water solution) were added to obtained solution and heated at 70 °C for 12 h. Then, the mixture was cooled to room temperature, and obtained white solid was filtered and washed with MeOH/water (1/1, v/v), and then dried at room temperature for 2 days (3: m.p.: 200 °C) [43].

Synthesis of 2-{4-[(2,2':6,2''-terpyridin)-4'-yl]phenoxy}ethyl acrylate 4. Acryloyl chloride (5.5 mmol, 0.5 g) was added drop wise to a cold solution of 3 (1.35 mmol, 0.5 g) and Et₃N (0.5 g) in 20 ml CHCl₃ in an ice bath, and stirred at the same temperature for 5 h. After completion of the reaction, the mixture was diluted with CH₂Cl₂ and washed with brine. Then, the organic was dried using anhydrous MgSO₄, and evaporated to give 4 as a light brown solid. M.p.: 132-134 °C; FT-IR (KBr) ν = 3051 (CH_{Ar}), 2928 (CH_{aliphatic}), 1727 (C=O), 1605, 1582, 1514 (C=C), 1399 (CH_{2-bending}), 1253, 1184 (C-O) cm⁻¹; ¹H NMR (CDCl₃, 400 MHz) δ = 4.32 (t, *J* = 4.8 Hz, 2H, CH₂), 4.59 (t, *J* = 4.8 Hz, 2H, CH₂), 5.89-5.92 (dd, *J* = 1.2, 10.4 Hz, CH_{vinyl}), 6.18-6.25 (dd, *J* = 10.4, 17.6 Hz, CH_{vinyl}), 6.48-6.52 (dd, *J* = 1.2, 17.6 Hz, CH_{vinyl}), 7.06-7.09 (m, 2H, CH_{Ar}), 7.37-7.40 (ddd, *J* = 1.2, 4.8, 7.6 Hz, 2H, CH_{Ar}), 7.89-7.93 (m, 4H, CH_{Ar}), 8.69 (d, *J* = 8.0 Hz, 2H, CH_{Ar}), 8.73 (s, 2H, CH_{Ar}), 8.75-8.77 (m, 2H, CH_{Ar}) ppm; ¹³C NMR (CDCl₃, 100 MHz) δ = 62.9, 66.0, 114, 118.2, 121.4, 123.8, 128.0, 128.6, 131.5, 136.9, 149.1, 149.6, 155.8, 156.3, 159.4, 166.1 (CO_{ester}) ppm.

Synthesis of 2-{4-[(2,2':6,2''-terpyridin)-4'-yl]phenoxy}ethyl-3-[(2-hydroxyethyl)amino]propanoate 5. MnCl₂·4H₂O was added to a solution of ethanol amine (1.11 mmol, 0.066 g) and 4 (1.11 mmol, 0.47 g) in 15 ml MeOH, and stirred at room temperature for 3 h. Then, the solvent was evaporated under reduced pressure, and obtained solid was washed with water. The yellow solid with m.p.: 140-143 °C was obtained [44].

Synthesis of graphene oxide. 400 ml solution of H₂SO₄/HNO₃ (9/1 v/v) was added to a mixture of graphite flakes (3.0 g) and KMnO₄ (18.0 g), and stirred at 50 °C for 12 h. After cooling to room temperature, 400 ml ice and 3 ml H₂O₂ (30%) was added to mixture, and the obtained solid was isolated by centrifuge at 4000 rpm, washed twice with DI water, three times with HCl 35%, and twice with EtOH. GO solution in water was obtained by ultrasonic irradiation for 20 min, followed by centrifuge at 5000 rpm for 10 min. The supernatant containing GO was isolated and stored at 4 °C for further uses [45].

Synthesis of GO-terpyridine conjugate (GOTC). 0.005 g GO was mixed with 10 ml SOCl₂ and heated under reflux at 70 °C for 24 h, and then the mixture was dried using rotary evaporator. The obtained solid was mixed with 5 (0.07 g) in 10 ml

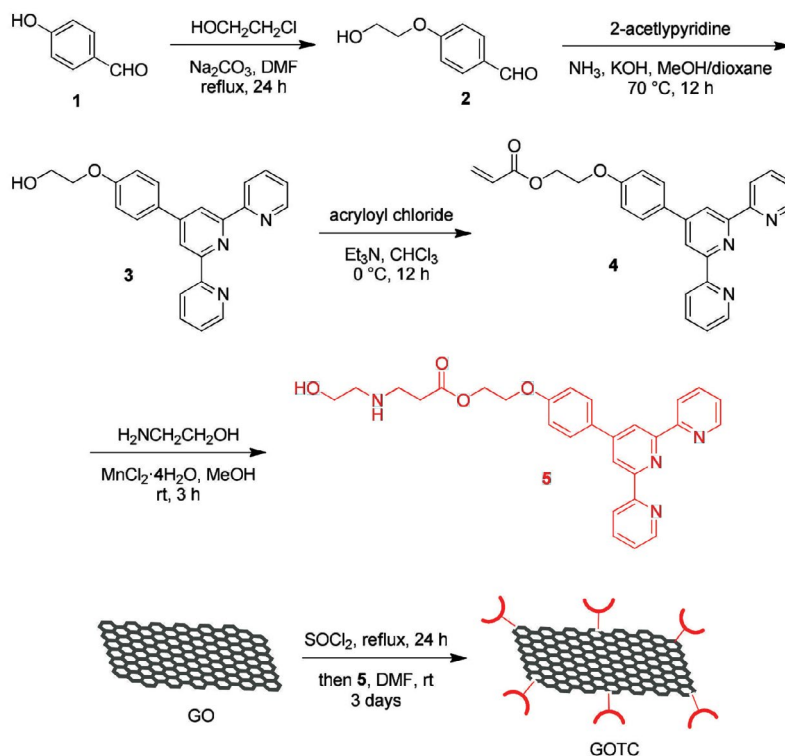
dry DMF and heated at 120 °C for 3 days. The solid was isolated by centrifuging at 4000 rpm for 10 min and washed with MeOH.

RESULTS AND DISCUSSION

Synthesis and Characterization of GOTC

The schematic representation of the synthesis of compound 5 and GOTC is shown in Scheme 1. The FT-IR of GO and GOTC is shown in Fig. 1, in which the O-H stretching vibration of GO was appeared as a broad signal at 3415 cm⁻¹, and C=O

of carboxylic acid groups was appeared at 1720 cm⁻¹. Peaks at 1621 and 1219 cm⁻¹ are related to the C=C and C-O stretching vibrations, respectively. In the FT-IR spectra of GOTC, O-H is appeared at 3415 cm⁻¹ as a broad peak, and the C-H stretching vibration of aromatic rings of 5 is appeared at 3062 cm⁻¹, and distinguished bands corresponding to the asymmetric and symmetric stretching modes of CH₂ groups of 5, are appeared at 2924 and 2853 cm⁻¹, respectively. Peak at 1726 cm⁻¹ is attributed to the stretching vibration of C=O of ester. Also, in



Scheme 1. Synthesis of GOTC

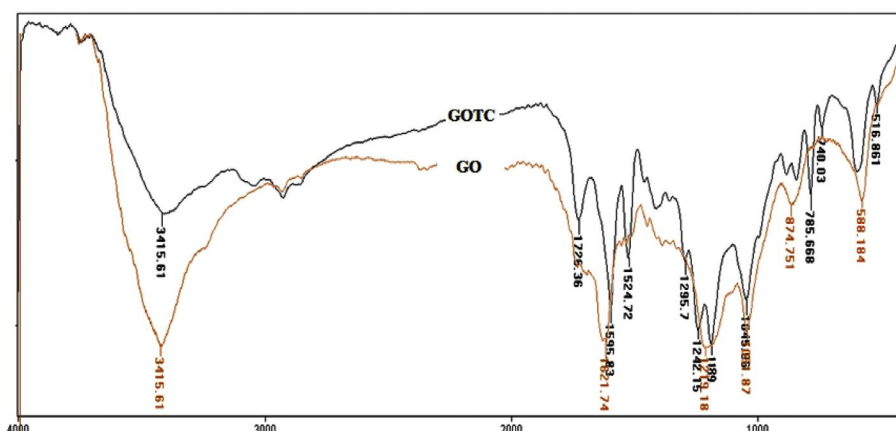


Fig. 1. FT-IR spectra of GO and GOTC.

the C=C bond region, in addition to C=C double bonds of GO at 1595 cm^{-1} , peaks at 1468 and 1525 cm^{-1} are attributed to the aromatic rings of phenyl and terpyridine moieties. Peak at 1413 cm^{-1} is related to the CH_2 bending vibration, and peaks at 1189, 1242 and 1296 cm^{-1} are attributed to C-O and C-N bond stretching vibrations, indicating the covalently linkage of 5 onto GO.

TEM image of an aqueous dispersion of GOTC (Fig. 2a) supported the existence of sheet like material, and revealed that the GOTC nanosheets are highly dispersed in water. Also, SEM image of GO shows single flakes of GO (Fig. 2b), which was shown as randomly aggregated crumpled sheets in the case of GOTC, indicating the modification on the surface of GO (Fig. 2c).

Colorimetric Fe^{2+} Sensing

Free GOTC (0.2 mg ml^{-1}) in water shows a weak absorption band centered at 568 nm. Upon addition of Fe^{2+} to GOTC solution (the final concentration of GOTC and Fe^{2+} are 0.2 mg ml^{-1} and $0.33 \mu\text{M}$, respectively), band at 568 nm increased, whereas addition of Fe^{3+} caused lower increase than Fe^{2+} at the band. Addition of Co^{2+} resulted in a weak absorption band centered at 516 nm, and in the case of other relevant metal ions, such as Li^+ , Na^+ , K^+ , Mg^{2+} , Ca^{2+} , Ba^{2+} , Al^{3+} , Ag^+ , Cu^{2+} , Pb^{2+} , Ni^{2+} , Mn^{2+} , Cd^{2+} , Hg^{2+} , Zn^{2+} and Cr^{3+} there are no any changes in the absorption spectra (Fig. 3). GOTC showed color changes from plum to dark magenta in the presence of Fe^{2+} and from plum to violet-red and yellow in the presence of Fe^{3+} and Co^{2+} , respectively,

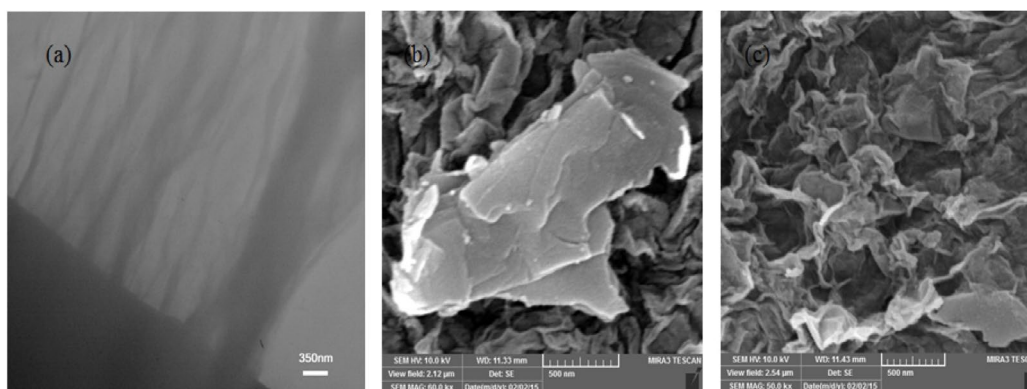


Fig. 2. TEM image of GOTC (a), and SEM images of GO (b) and GOTC (c).

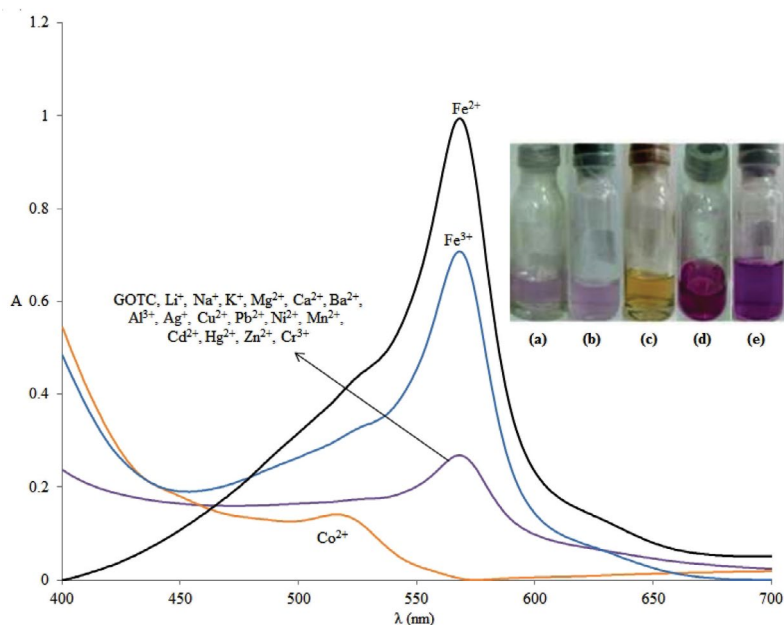


Fig. 3. The color changes of GOTC upon addition of various metal ions: (a) free GOTC (0.2 mg ml^{-1}), (b) after addition of relevant metal ions (Li^+ , Na^+ , K^+ , Mg^{2+} , Ca^{2+} , Ba^{2+} , Al^{3+} , Ag^+ , Cu^{2+} , Pb^{2+} , Ni^{2+} , Mn^{2+} , Cd^{2+} , Hg^{2+} , Zn^{2+} and Cr^{3+}), (c) Co^{2+} , (d) Fe^{3+} and (e) Fe^{2+} .

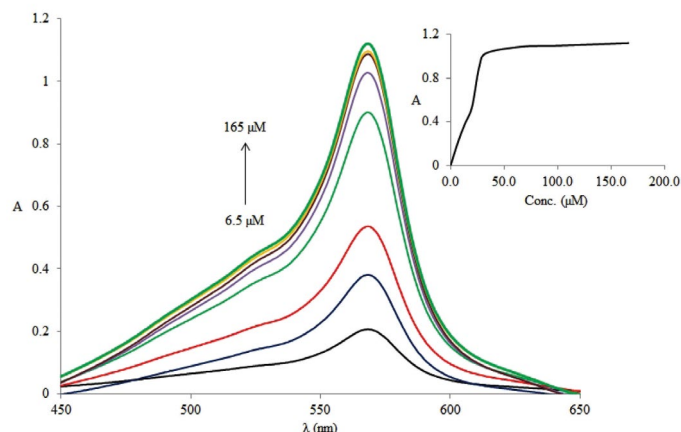


Fig. 4. Titration of GOTC with Fe^{2+} .

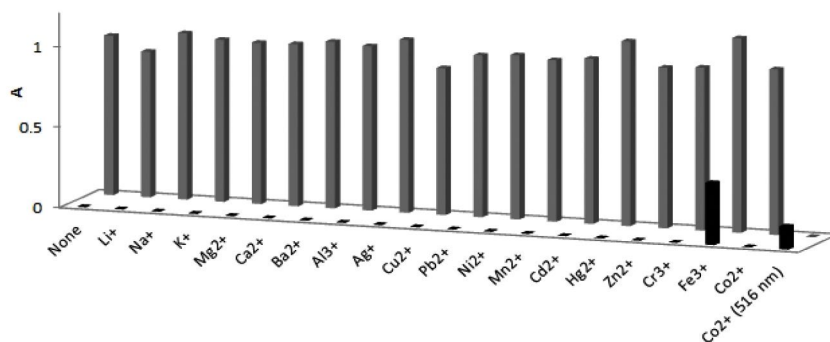


Fig. 5. Competitive metal ion titrations with Fe^{2+} , absorbance is at 568 nm, unless that is mentioned, black bars: absorbance of a solution of GOTC (0.2 mg ml^{-1}) + metal ions ($0.33 \text{ } \mu\text{M}$), gray bars: absorbance of a solution of GOTC (0.2 mg ml^{-1}) + metal ions ($0.33 \text{ } \mu\text{M}$) + Fe^{2+} ($0.33 \text{ } \mu\text{M}$); data in parenthesis are the final concentration in 3 ml solution).

while other metal ions caused no change in color (Fig. 3, inset). Upon titration of GOTC with Fe^{2+} , the absorbance at 568 nm increased sharply (Fig. 4), which may be attributed to the interaction of Fe^{2+} ions with the terpyridyl moiety leading to the metal-to-terpyridine-charge-transfer. Whereas, the increasing of Fe^{3+} and Co^{2+} concentration caused little increase at the corresponding bands at 586 nm and 516 nm, respectively.

In order to investigate the practical utility of GOTC to detect Fe^{2+} ions selectively in the presence of other metal ions, competitive metal ion titrations were carried out by titration of a solution of GOTC and different metal ions with Fe^{2+} . In the case of Co^{2+} , the absorption band at 516 nm disappeared, while absorbance at 568 nm increased as a function of the addition of Fe^{2+} . By addition of Fe^{2+} to a solution of Fe^{3+} and GOTC, a little change was observed at 568 nm at low concentrations of Fe^{2+} , but increased when the concentration of Fe^{2+} reached to the Fe^{3+} ones. In all other cases absorbance at 568 nm increased as a function of the addition of Fe^{2+} (Fig. 5).

Due to the distinct color change of GOTC upon addition of Fe^{2+} solution, and to obtain a naked-eye detection method, the sensing on the test paper was also investigated by immersing a piece of filter paper into a sensor solution, followed by drying under vacuum at $50 \text{ } ^\circ\text{C}$. By immersing the obtained test paper into the solution of various metals ions, no color changes were observed, except for Fe^{2+} solution, which led to the color change from light pink to magenta. However, in the case of Fe^{3+} solution, the slightly yellowish color was observed (Fig. 6).

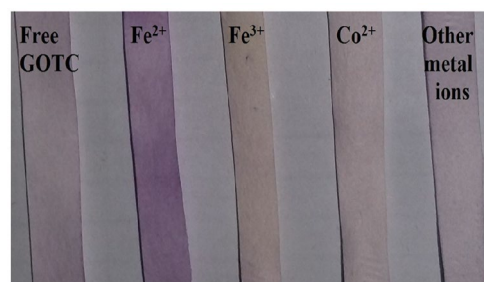


Fig. 6. Paper sensing of Fe^{2+} ions.

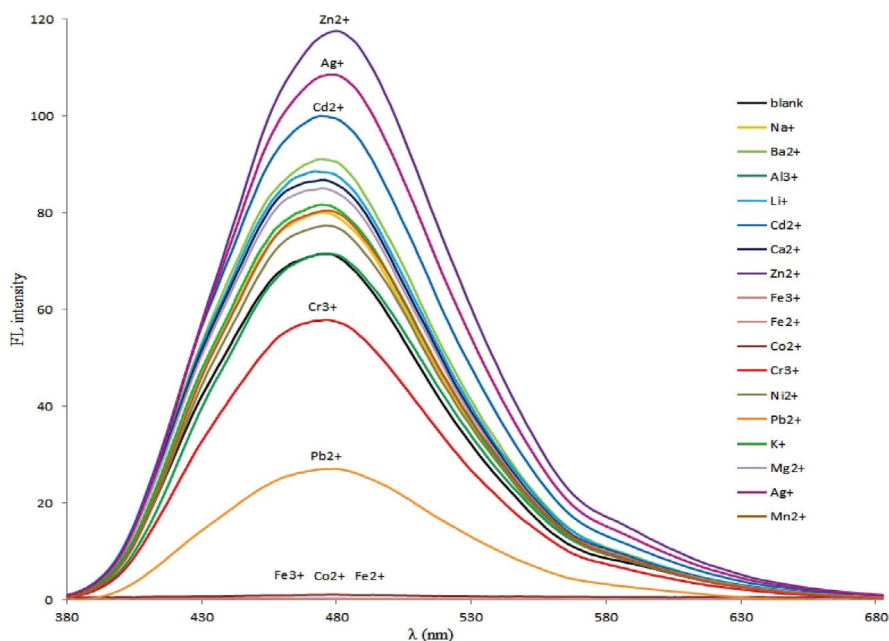


Fig. 7. Fluorescence of GOTC (0.2 mg ml⁻¹) upon addition of various metal ions (0.33 μM).

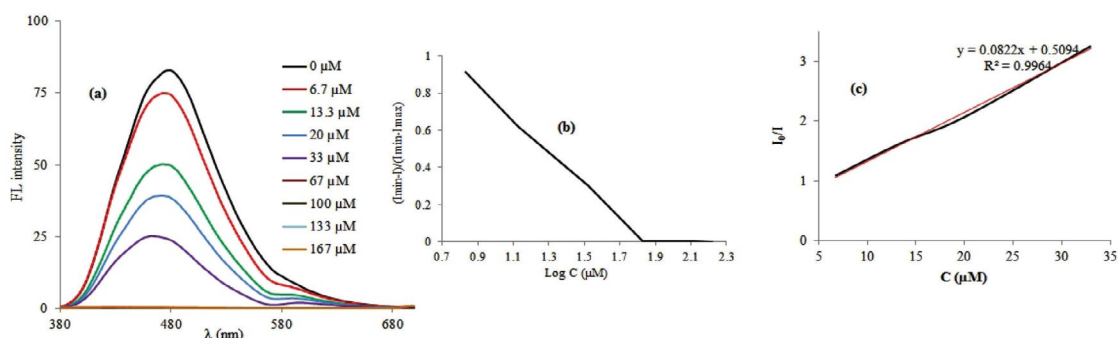


Fig. 8. Fluorescence intensity of GOTC upon titration with Fe²⁺ (a), the normalized intensity $[(I_{\min} - I)/(I_{\min} - I_{\max})]$ plot against $\log C$ (μM) of Fe²⁺ (b), and Stern-Volmer plot for GOTC in the presence of Fe²⁺ (c).

Fluorescence Fe²⁺ Sensing

The fluorescence response behavior of GOTC was examined upon treatment with various metal ions in water. Fig. 7 shows that the addition of Li⁺, Na⁺, K⁺, Mg²⁺, Ca²⁺, Ba²⁺, Al³⁺, Ni²⁺, Mn²⁺ causes a little fluorescence increase, and the addition of Cd²⁺, Ag⁺ and Zn²⁺ results in a pronounced fluorescence enhancement, whereas addition of Cr³⁺ and Pb²⁺ leads to a decrease in fluorescence of GOTC, and the addition of Fe²⁺, Fe³⁺ and Co²⁺ causes full quenching of the fluorescence of GOTC. To determine the sensitivity range of GOTC toward Fe²⁺, the fluorescence properties of GOTC were investigated upon addition of different amounts of Fe²⁺ (Fig. 8a). The normalized intensity $[(I_{\min} - I)/$

$(I_{\min} - I_{\max})]$ was plotted against $\log C$ (μM) of Fe²⁺, which exhibited good linearity in the range of 6.5×10^{-6} M- 67×10^{-6} M (Fig. 8b). The most abundant complex formed within the range of 6.5-33 μM of Fe²⁺, showed a 1:1 (host/guest) stoichiometry, using the Stern-Volmer plot, as shown in Fig. 8c.

CONCLUSIONS

In summary, a nano-chemical sensor for Fe²⁺ ions was developed based on terpyridine conjugated on GO. Both colorimetric and fluorescence method were investigated, in which the sensor exhibited good linearity in the range of 6.5×10^{-6} - 33×10^{-6} M and 6.5×10^{-6} M- 67×10^{-6} M, respectively. Also, competitive metal ion titrations

were carried out, that exhibited best selectivity for Fe²⁺ ions. The solubility of designed sensor in water is an important advantage, leading to detection of Fe²⁺ ions in aqueous solution.

ACKNOWLEDGEMENTS

The work was supported by research council of the University of Maragheh. B. Eftekhari-Sis thanks Prof. A. Jouyban (Drug Applied Research Centre, Tabriz University of Medical Sciences) for fluorescent spectra.

REFERENCES

- [1] De Silva AP, Gunaratne HN, Gunnlaugsson T, Huxley AJ, McCoy CP, Rademacher JT, et al. Signaling recognition events with fluorescent sensors and switches. *Chem. Rev.* 1997; 97 (5): 1515-66.
- [2] Quang DT, Kim JS. Fluoro-and chromogenic chemodosimeters for heavy metal ion detection in solution and biospecimens. *Chem. rev.* 2010; 110 (10): 6280-301.
- [3] Czarnik AW. Chemical communication in water using fluorescent chemosensors. *Acc. Chem. Res.* 1994; 27 (10): 302-8.
- [4] Valeur B, Leray I. Design principles of fluorescent molecular sensors for cation recognition. *Coord. Chem. Rev.* 2000; 205 (1): 3-40.
- [5] Ranyuk E, Douaihy CM, Bessmertnykh A, Denat F, Averin A, Beletskaya I, et al. Diaminoanthraquinone-linked polyazamacrocycles: efficient and simple colorimetric sensor for lead ion in aqueous solution. *Org. Lett.* 2009; 11 (4): 987-90.
- [6] Wang S, Chen Z, Chen L, Liu R, Chen L. Label-free colorimetric sensing of copper(II) ions based on accelerating decomposition of H₂O₂ using gold nanorods as an indicator. *Analyst.* 2013; 138 (7): 2080-4.
- [7] Basurto S, Riant O, Moreno D, Rojo J, Torroba T. Colorimetric Detection of Cu(II) Cation and Acetate, Benzoate, and Cyanide Anions by Cooperative Receptor Binding in New α , α' -Bis-substituted Donor-Acceptor Ferrocene Sensors. *J. Org. Chem.* 2007; 72 (13): 4673-88.
- [8] Zhou H, Tian W, Jiang M, Li P, Zeng S, Chen W, et al. A Selective, Colorimetric and Ratiometric Chemosensor for Hg²⁺ and Its Application as Test Papers. *Anal. Sci.* 2015; 31 (12): 1285-9.
- [9] Li S-H, Yuan W-T, Zheng H, XU J-G. Colorimetric recognition of different enzymology-concerning transition metals based on a hybrid cluster complex. *Anal. Sci.* 2004; 20 (7): 997-9.
- [10] Jung HS, Kwon PS, Lee JW, Kim JI, Hong CS, Kim JW, et al. Coumarin-derived Cu²⁺-selective fluorescence sensor: synthesis, mechanisms, and applications in living cells. *J. Am. Chem. Soc.* 2009; 131 (5): 2008-12.
- [11] Kim HN, Lee MH, Kim HJ, Kim JS, Yoon J. A new trend in rhodamine-based chemosensors: application of spirolactam ring-opening to sensing ions. *Chem. Soc. Rev.* 2008; 37 (8): 1465-72.
- [12] Zhang JF, Kim JS. Small-molecule fluorescent chemosensors for Hg²⁺ ion. *Anal. Sci.* 2009; 25 (11): 1271-81.
- [13] Qi X, Jun EJ, Xu L, Kim S-J, Joong Hong JS, Yoon YJ, et al. New BODIPY derivatives as off-on fluorescent chemosensor and fluorescent chemodosimeter for Cu²⁺: cooperative selectivity enhancement toward Cu²⁺. *J. Org. Chem.* 2006; 71 (7): 2881-4.
- [14] Kawakami J, Ohta M, Yamauchi Y, Ohzeki K. 8-Hydroxyquinoline derivative as a fluorescent chemosensor for zinc ion. *Anal. Sci.* 2003; 19 (10): 1353-4.
- [15] Zeng Y, Zhang G, Zhang D. A Tetraphenylethylene-based Fluorescent Chemosensor for Cu²⁺ in Aqueous Solution and Its Potential Application to Detect Histidine. *Anal. Sci.* 2015; 31 (3): 191-5.
- [16] Weizman H, Ardon O, Mester B, Libman J, Dvir O, Hadar Y, et al. Fluorescently-labeled ferrichrome analogs as probes for receptor-mediated, microbial iron uptake. *J. Am. Chem. Soc.* 1996; 118 (49): 12368-75.
- [17] Sumner JP, Kopelman R. Alexa Fluor 488 as an iron sensing molecule and its application in PEBBLE nanosensors. *Analyst.* 2005; 130 (4): 528-33.
- [18] Lynch SR. Interaction of iron with other nutrients. *Nutr. Rev.* 1997; 55 (4): 102-10.
- [19] Rouault TA. The role of iron regulatory proteins in mammalian iron homeostasis and disease. *Nat. Chem. Biol.* 2006; 2 (8): 406-14.
- [20] Zhang X-B, Cheng G, Zhang W-J, Shen G-L, Yu R-Q. A fluorescent chemical sensor for Fe³⁺ based on blocking of intramolecular proton transfer of a quinazolinone derivative. *Talanta.* 2007; 71 (1): 171-7.
- [21] Bricks JL, Kovalchuk A, Trieflinger C, Nofz M, Büschel M, Tolmachev AI, et al. On the development of sensor molecules that display Fe(III)-amplified fluorescence. *J. Amer. Chem. Soc.* 2005; 127 (39): 13522-9.
- [22] Mao J, Wang L, Dou W, Tang X, Yan Y, Liu W. Tuning the selectivity of two chemosensors to Fe(III) and Cr(III). *Org. Lett.* 2007; 9 (22): 4567-70.
- [23] Lee MH, Van Giap T, Kim SH, Lee YH, Kang C, Kim JS. A novel strategy to selectively detect Fe(III) in aqueous media driven by hydrolysis of a rhodamine 6G Schiff base. *Chem. Commun.* 2010; 46 (9): 1407-9.
- [24] Wang B, Hai J, Liu Z, Wang Q, Yang Z, Sun S. Selective Detection of Iron (III) by Rhodamine-Modified Fe₃O₄ Nanoparticles. *Angew. Chem. Int. Ed.* 2010; 49 (27): 4576-9.
- [25] Oter O, Ertekin K, Kirilmis C, Koca M, Ahmedzade M. Characterization of a newly synthesized fluorescent benzofuran derivative and usage as a selective fiber optic sensor for Fe(III). *Sens. Actuator B-Chem.* 2007; 122 (2): 450-6.
- [26] Zhan J, Wen L, Miao F, Tian D, Zhu X, Li H. Synthesis of a pyridyl-appended calix [4] arene and its application to the modification of silver nanoparticles as an Fe³⁺ colorimetric sensor. *New J. Chem.* 2012; 36 (3): 656-61.
- [27] Fan L-J, Jones WE. A highly selective and sensitive inorganic/organic hybrid polymer fluorescence "turn-on" chemosensory system for iron cations. *J. Amer. Chem. Soc.* 2006; 128 (21): 6784-5.

- [28] Huang WT, Xie WY, Shi Y, Luo HQ, Li NB. A simple and facile strategy based on Fenton-induced DNA cleavage for fluorescent turn-on detection of hydroxyl radicals and Fe²⁺. *J. Mater. Chem.* 2012; 22 (4): 1477-81.
- [29] Liang Z-Q, Wang C-X, Yang J-X, Gao H-W, Tian Y-P, Tao X-T, et al. A highly selective colorimetric chemosensor for detecting the respective amounts of iron(II) and iron(III) ions in water. *New J. Chem.* 2007; 31 (6): 906-10.
- [30] Zheng M, Tan H, Xie Z, Zhang L, Jing X, Sun Z. Fast Response and High Sensitivity Europium Metal Organic Framework Fluorescent Probe with Chelating Terpyridine Sites for Fe³⁺. *ACS Appl. Mater. Interfaces.* 2013; 5 (3): 1078-83.
- [31] Postma HWC. Rapid sequencing of individual DNA molecules in graphene nanogaps. *Nano Lett.* 2010; 10 (2): 420-5.
- [32] He S, Song B, Li D, Zhu C, Qi W, Wen Y, et al. A graphene nanoprobe for rapid, sensitive, and multicolor fluorescent DNA analysis. *Adv. Funct. Mater.* 2010; 20 (3): 453-9.
- [33] Guo Y, Deng L, Li J, Guo S, Wang E, Dong S. Hemin-graphene hybrid nanosheets with intrinsic peroxidase-like activity for label-free colorimetric detection of single-nucleotide polymorphism. *ACS nano.* 2011; 5 (2): 1282-90.
- [34] Wu W, Hu H, Li F, Wang L, Gao J, Lu J, et al. A graphene oxide-based nano-beacon for DNA phosphorylation analysis. *Chem. Commun.* 2011; 47 (4): 1201-3.
- [35] Song Y, Qu K, Zhao C, Ren J, Qu X. Graphene oxide: intrinsic peroxidase catalytic activity and its application to glucose detection. *Adv. Mater.* 2010; 22 (19): 2206-10.
- [36] Tan X, Chen T, Xiong X, Mao Y, Zhu G, Yasun E, et al. Semiquantification of ATP in live cells using nonspecific desorption of DNA from graphene oxide as the internal reference. *Anal. Chem.* 2012; 84 (20): 8622-7.
- [37] Chang H, Tang L, Wang Y, Jiang J, Li J. Graphene fluorescence resonance energy transfer aptasensor for the thrombin detection. *Anal. Chem.* 2010; 82 (6): 2341-6.
- [38] Wang L, Pu KY, Li J, Qi X, Li H, Zhang H, et al. A Graphene-Conjugated Oligomer Hybrid Probe for Light-Up Sensing of Lectin and Escherichia Coli. *Adv. Mater.* 2011; 23 (38): 4386-91.
- [39] Yang W, Ratinac KR, Ringer SP, Thordarson P, Gooding JJ, Braet F. Carbon nanomaterials in biosensors: should you use nanotubes or graphene?. *Angew. Chem. Int. Ed.* 2010; 49 (12): 2114-38.
- [40] Li D, Kaner RB. Graphene-based materials. *Nat. Nanotechnol.* 2008; 3: 101.
- [41] Eftekhari-Sis B, Ghahramani F. Synthesis of 2-[5-[4-((4-nitrophenyl) diazenyl) phenyl]-1, 3, 4-oxadiazol-2-ylthio] ethyl acrylate monomer and its application in a dual pH and temperature responsive soluble polymeric sensor. *Des Monomers Polym.* 2015; 18 (5): 460-9.
- [42] Mao PC-M, Mouscadet J-F, Leh H, Auclair C, Hsu L-Y. Chemical modification of coumarin dimer and HIV-1 integrase inhibitory activity. *Chem. Pharm. Bull.* 2002; 50 (12): 1634-7.
- [43] Tu S, Jia R, Jiang B, Zhang J, Zhang Y, Yao C, et al. Kröhnke reaction in aqueous media: one-pot clean synthesis of 4'-aryl-2, 2': 6', 2''-terpyridines. *Tetrahedron.* 2007; 63 (2): 381-8.
- [44] Roy A, Kundu D, Kundu SK, Majee A, Hajra A. Manganese(II) Chloride-Catalyzed Conjugated Addition of Amines to Electron Deficient Alkenes in Methanol-Water Medium. *TOCATJ.* 2010; 3 (1).
- [45] Marcano DC, Kosynkin DV, Berlin JM, Sinitskii A, Sun Z, Slesarev A, et al. Improved synthesis of graphene oxide. *ACS nano.* 2010; 4 (8): 4806-14.